

# Similarity Estimation on Ancient Vessels

Christian Hörr\* Guido Brunnett†  
Chemnitz University of Technology, Germany



Figure 1: Most similar vessels chosen from 300 datasets by objective weighting of automatically extracted shape features

## Abstract

Within archaeology inconsistent documentation styles and classification schemes have ever prevented the scientific work from being comprehensible and reproducible. Now that the advantages of 3D scanning technology become more and more evident, it is possible for the first time to exclude subjective influences and to make new attempts for an overdue standardization. As a first step, we show how morphological features can be extracted automatically from 3D scanned pottery, including not only heights and diameters but also ratios and other major properties such as handles and feet for example. These features are then used to estimate the similarity between arbitrary vessels. At first, we therefore propose similarity metrics for different kinds of features. Afterwards the importance of features is ranked by the gain ratio criterion from the well-known C4.5 decision tree algorithm which is finally used to set the particular weights for the computation of the overall similarity. The good query results obtained on Bronze Age material confirm our presumption that the method is applicable in many other domains too.

**Keywords:** archaeological pottery, shape analysis, mesh segmentation, similarity metric, gain ratio.

## 1 Problem Statement

Archaeology is specifically a perception-based and comparative science and so one of the major tasks in archaeological research is the search for similar entities. This process usually includes but is not limited to morphological analysis. Together with secondary attributes such as treatment, texture or material functional, behavioural and finally chronological conclusions can be drawn. Probably the most important group among findings is formed by ceramic vessels. Besides from being the far biggest part of all artifacts, they also give good clues about the life and cults of their ancient manufacturers. Moreover, the special axially symmetric shape of vessels makes them predestined for automatic analysis and the induction of typologies.

Although there have already been many approaches towards a standardized classification process, none of them could prevail so far [Whallon and Brown 1982; Adams and Adams 1991]. For the first time, 3D range scanning technology allows for an objective reproduction of reality and for the acquisition and processing of incomparable greater quantities of data. Since classification in archaeology is usually based on unstandardized manual drawings, the search

for similar objects has always been biased by several human influences. For that reason, archaeologists always longed for methods quantifying similarities more objectively and in particular making the proceeding comprehensible and reproducible. As a first step, in [Hörr et al. 2008a] we propose several non-photorealistic rendering styles heading for uniform drawing conventions. We have also shown that in the domain of pottery machine learning techniques are very suitable for the reliable prediction of primary and even secondary types solely on the basis of feature values, but also for verification and refinement of existing typologies [Hörr et al. 2008b].

In the following, algorithms are presented that compute the most relevant morphological features automatically from the 3D models of axially symmetric vessels in order to accelerate data acquisition even more. Section 2 is commenced by the computation of profiles, the most important measures and their ratios. Later we present a fast and straightforward algorithm to detect body extensions like handles, lugs and feet. As well, we make proposals for the computation of a representative average profile which may serve for further analysis. How the extracted features can be processed in user-defined queries is the topic of section 3. There, similarity metrics for numerical and nominal features are introduced and it is shown that an objective weighting of features is possible by calculating their importance using the gain ratio criterion from the C4.5 algorithm [Quinlan 1993]. Section 4 is dedicated to some results and general observations that may support the daily typological work of archaeologists.

## Related Work

During the past years there have been many new attempts towards shape matching. These include, among others, topological ones [Hilaga et al. 2001], skeleton-based ones [Brennecke and Isenberg 2004; Cornea et al. 2005], shape histograms [Ankerst et al. 1999] and feature vectors [Bustos et al. 2005]. Almost all of them consider similarity as a global measure and hence perform best on a diversity of object classes. If however differences in detail are to be discovered, most of them fail. Moreover, 3D scanned vessels do not meet the requirements of the majority of existing algorithms. This applies also for spectral analysis (e.g. [Reuter et al. 2007]), because a uniform mesh topology as well as suitable boundary conditions cannot be assured if for example parts of the surface, particularly inner walls are missing. We therefore believe that for the special domain of pottery a specific non-global feature-based approach is much more flexible and convenient.

Gilboa et al. [2004] developed methods for deriving a vessel typology by comparing the profiles of rim sherds. They understand similarity as the correlation of parametrizations of the profile curve.

\*hoerr@cs.tu-chemnitz.de

†brunnett@cs.tu-chemnitz.de

However, this approach is suitable only to determine type membership and it fails if profiles of complete vessels are considered. In [Saragusti et al. 2005] Fourier analysis is used to describe the roughness and symmetry of horizontal cross sections of pots or contours of handaxes. Kampel and Sablatnig [2007] apply classification rules established empirically by archaeological experts to assign sherds to a certain vessel type, but it remains unclear what the system’s contribution is, if the human’s typology is merely reproduced and not questioned. Moreover, the presented rules are not generalizable and tests were carried out only on very few sherds.

## 2 Feature Extraction

Whether wheel-thrown or handcrafted, throughout history the very most vessels have been designed as rotational bodies. We take advantage of this special property by first aligning the vessels with their estimated axis of rotation (a new symmetry-based algorithm is presented in [Wagner 2007]) and then transforming them into a cylindrical coordinate system where points are described in terms of height  $h$ , radius  $r$  and angle  $\varphi$ . If the vessel is indeed totally axially symmetric,  $r$  is constant with respect to a specified height and the angle dimension becomes redundant. Therefore, archaeologists usually describe features of vessels only as features of a certain representative half profile, although ancient pottery is often distorted for reasons of manufacturing, burning and storing. Hence, immediately the question arises how such a profile should look like and how it is computed.

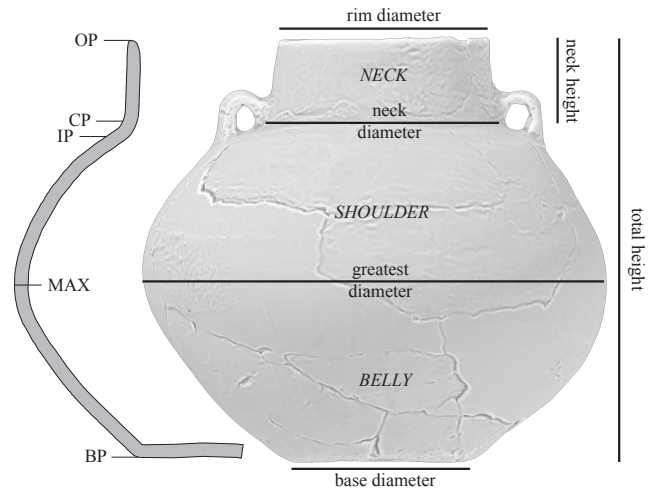
### 2.1 Fast Computation of Profiles

In general, profiles are computed by an intersection of the vessel with half-planes whose borders are the axis of rotation. However, doing this for a large number on triangular meshes is computationally expensive. Therefore we propose a different approach which is based on a discretized cylindrical mapping. We subdivide the vertical axis (the height axis) into  $I$  and the angle axis into  $J$  intervals resulting in an  $I \times J$  2D-grid around the axis of rotation.  $I$  is chosen with respect to the object’s height so that each row of the grid covers approximately 1-2 millimeters. For  $J$  it has turned out that a resolution of one degree per column is far sufficient, so  $J$  is constantly set to 360.

Now, each mesh vertex can be projected into exactly one of the cells according to its  $h$  and  $\varphi$  coordinates. If its distance value  $r$  is greater than the already stored one it is written to that cell. The storage of only the maximum distance values is reasonable because for the vessel’s shape analysis only the outer surface is of interest and since multiple values are precluded, computation is much simplified. Finally a  $2\frac{1}{2}$ -dimensional grid evolves where in the following rows are called *slices* and columns are called *profiles*. The set of all distance values within a fixed slice is referred to as *distance function*  $d(\varphi)$  of that slice (fig. 3(a)). This function is periodic and might be partially undefined, if some cells are empty, e.g. due to missing pieces of the vessel. In this case gaps are simply closed via linear interpolation. As stated above, for a perfectly symmetric rotational body the distance function is expected to be constant. In practice however, due to distortion or imprecise alignment it changes to a more or less sinusoidal oscillation. Moreover, if the surface is rough or decorated, noise and small bumps appear. For further analysis the distance function is slightly smoothed.

### 2.2 Measures, Ratios and Body Segments

In documentation of archaeological pottery, aside from the description of colour, material, burning and state of preservation the most important geometric measures are denoted. These include the total height, the maximum diameter, the diameters of the base and



**Figure 2:** Characteristic profile points and most important measures of a Bronze Age amphora.

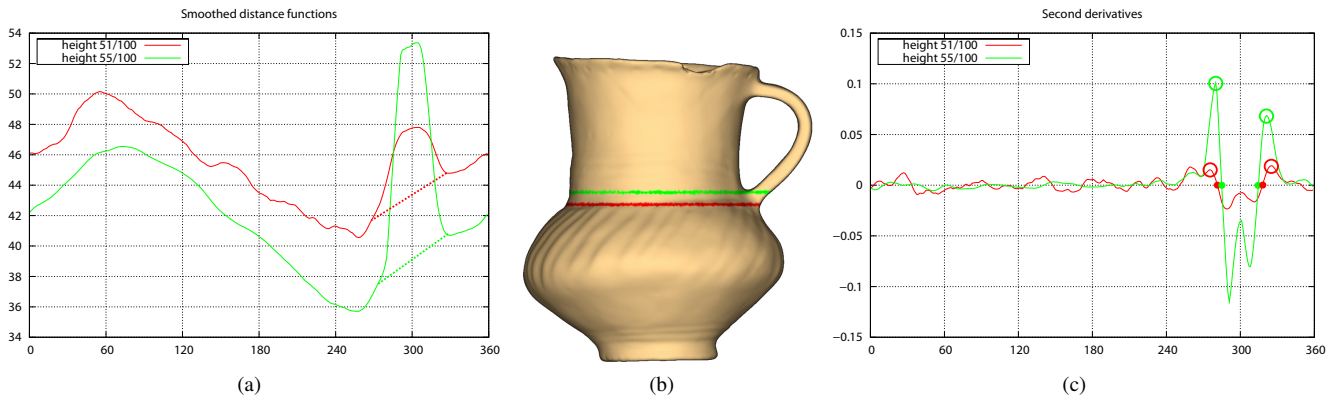
the rim, and sometimes also the diameter of the neck. The diameters are usually taken at characteristic points of the profile (fig. 2, first described in [Birkhoff 1933]) such as points of vertical tangency (MIN/MAX), corner points (CP), inflection points (IP) and the base (BP) and orifice point (OP). Identifying those points on a single profile is rather simple, especially if attachments have been excluded before (see following section). For a more precise analysis we compute best fitting circles among the corresponding characteristic points on all profiles. This provides us results being more independent from correct alignment as well as a measure of how much the corresponding diameters vary (uniformity, cf. [Mara et al. 2004; Saragusti et al. 2005]).

The characteristic profile points also indicate the borders of the body segments base, belly, shoulder, neck and rim. From that it is easy to conclude to the composition of body segments. On our material the shapes are limited to belly–rim (BR; simple bowls, porringers, flat cups), belly–shoulder–rim (BSR; esp. double-cones) and belly–shoulder–neck–rim (BSNR; amphorae, tureens, profiled cups). To distinguish simple bowls from profiled bowls we also introduced the special shape BRp. Our experiments have shown that this semantic approach is much more suitable than a geometric curve matching of profiles, the comparison of the sequence of characteristic profile points (the profile signature) or the mapping of body segments to geometric primitives (e.g. [Rice 1987, 219]).

Since uniform scaling is usually irrelevant to the upper levels of vessel typologies, i.e. size does not matter, instead of absolute measures in most cases some selected ratios of them are far more meaningful. Some of the most important ones are

$$\begin{aligned} \text{main index} &= 100 \cdot \frac{\text{greatest diameter}}{\text{total height}}, \\ \text{rim index} &= 100 \cdot \frac{\text{rim diameter}}{\text{greatest diameter}}, \\ \text{neck index} &= 100 \cdot \frac{\text{rim diameter} - \text{neck diameter}}{2 \cdot \text{neck height}}, \\ \text{shoulder index} &= 100 \cdot \frac{\text{belly diameter} - \text{neck diameter}}{2 \cdot \text{shoulder height}}, \\ \text{base index} &= 100 \cdot \frac{\text{belly diameter} - \text{base diameter}}{2 \cdot \text{belly height}}. \end{aligned}$$

Multiplying them with 100 is only for better reading. Together with



**Figure 3:** Distance functions and their second derivatives of two cross sections

the relative heights of the belly and neck diameters these ratios already give a good impression of how the vessel’s body approximately looks like. Within a group of similar vessels their averages (or better medians) might also represent a reasonable prototype.

### 2.3 Detecting Attachments

An at least equally important question is if there are handles and other elements being attached to the body, because the existence of such attachments has a strong implication on the vessel’s intended purpose. Obviously, appendages violate the rotational symmetry and the corresponding profiles differ significantly from those on the rest of the body. This becomes even clearer if we consider the distance functions of slices that intersect those appendages (fig. 3). They contain one or more clearly observable peaks that superimpose the basic oscillation. Although in general these peaks are not sinusoidal, we can also speak of them as oscillations, but with a much higher frequency than the basic one. The problem of finding attachments can thus be reduced to the detection of peaks that cannot be explained by a low-swinging distance function. An attachment is detected if the following three conditions hold.

**Condition 1:** Finding the parameters of the basic oscillation for subsequent subtraction from the distance function is sometimes difficult, especially when attachment peaks coincide with its minimum and/or maximum. In fact however we don’t even depend on these parameters if we just analyze the occurrence of the distance function’s inflection points. Every perfect oscillation has two of them within one period with an offset of half the period. In case of our basic oscillation this offset should roughly be 180 degrees. However, an oscillation of a much higher frequency causes the offset to be clearly smaller, what is going to be our first condition for the existence of an attachment.

**Condition 2:** Because the basic oscillation is not exactly sinusoidal and besides that noise can bias the second derivative a lot, the actual number of inflection points can become rather high. Therefore we make use of a second observation which basically says that the distance function’s curvature is largest where unexpected peaks start and end (fig. 3(c)). To be considered significant over noise these maxima need to exceed the standard deviation of the second derivative and they both need to be in direct neighbourhood of an inflection point found by the first condition.

**Condition 3:** Once the potentially start and end angles  $\varphi_1$  and  $\varphi_2$  are found, it has to be checked if the corresponding peak in the distance function is indeed significant. We therefore replace the distance function between  $\varphi_1$  and  $\varphi_2$  with a function  $\bar{d}(\varphi)$  (dotted

lines in fig. 3(a)). In general, a linear function should suffice, but of course more sophisticated techniques such as Hermite or spline interpolation serve even better. Finally, an attachment is detected if the area  $A$  enclosed by the distance function and the interpolating function exceeds a certain threshold which depends on the level of detected noise.

$$A = \int_{\varphi_1}^{\varphi_2} (d(\varphi) - \bar{d}(\varphi)) d\varphi \quad (1)$$

In order to choose this threshold as low as possible we also make use of the property that the starting and end angles  $\varphi_1$  and  $\varphi_2$  should be coherent among adjacent slices. Hence, also the small hill in the upper distance function of fig. 3(a) could have been detected.

### Bails and Feet

In some periods bails and feet may have been mounted to the vessel’s body. However, these as well as rim-standing handles cannot be detected by the presented algorithm, because above and below the body the distance function cannot be assumed to be constant. Therefore, every segment that lies below the base plane or above the orifice plane is treated as an attachment by default. The computation of these planes can easily be performed by means of the base and orifice points described above.

### Implementation Details

In the current implementation of the presented algorithm the distance function is preprocessed with a Laplacian filter for smoother derivatives. The derivatives themselves are approximated discretely by the difference quotient. Inflection points are found by the change of signs.

After the attachments have been correctly detected, a mesh-grid-association is simple. However, due to the cylindrical projection body vertices that are projected into an attachment cell have to be excluded. This could for example be done by adding a small threshold to the interpolation function  $\bar{d}(\varphi)$  and testing the vertices’ radii against that function.

In case of plastic ornamentations or little bumps sometimes the noise analysis fails and very small pseudo-attachments are computed. To treat this, a minimum size for body extensions is demanded.

As the results in fig. 4 show, the algorithm is at the same time robust and precise. Since all computation is performed on a discrete

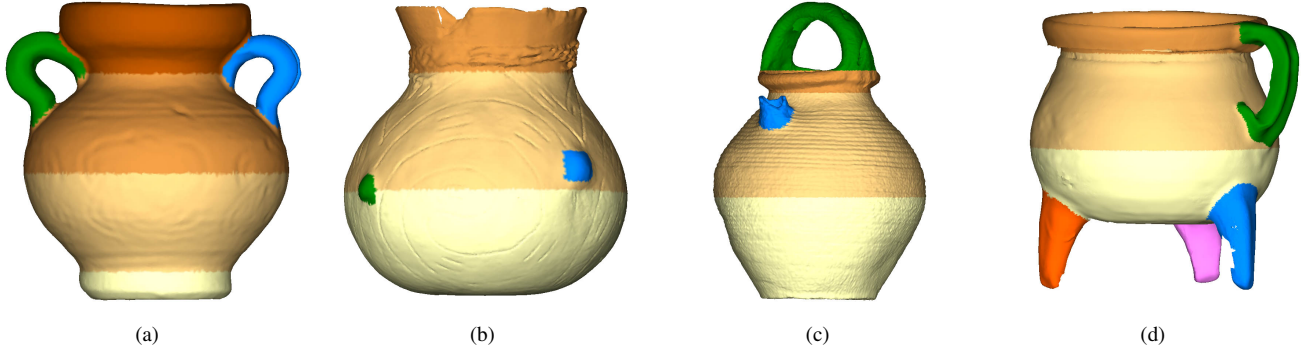


Figure 4: Segmentation of vessels from different eras

**Algorithm 1** Detecting attachments by means of edges within the distance function

- 1: compute all profiles and distance functions by cylindrical projection
- 2: close holes in the distance function by linear interpolation
- 3: compute characteristic profile points
- 4: compute first and second derivatives of the distance function
- 5: **for all** slices in  $h$  **do**
- 6:   **for all** profiles in  $\varphi$  **do**
- 7:     **if**  $d''(\varphi) = 0$  **and**  $d'(\varphi) > 0$  **then** // rising edge
- 8:       find previous local maximum in  $d''$  at  $\varphi_1$
- 9:     **else if**  $d''(\varphi) = 0$  **and**  $d'(\varphi) < 0$  **then** // falling edge
- 10:       find next local maximum in  $d''$  at  $\varphi_2$
- 11:     **end if**
- 12:     **if**  $\varphi_2 - \varphi_1 < \pi/2$  **and** integral exceeds threshold **then**
- 13:       attachment detected
- 14:     **end if**
- 15:   **end for**
- 16: **end for**
- 17: delete pseudo-attachments and exclude body-related vertices

grid whose resolution is usually much smaller than the point cloud density the whole algorithm has a complexity of only  $\mathcal{O}(n)$  with  $n$  denoting the number of mesh vertices. Indeed, only the mesh-grid-discretization step is predominant. Thus, even for large objects with more than 1,000,000 vertices the computation time does not exceed a few seconds.

## 2.4 The Optimal Profile

By the exclusion of attachments the estimation of an average profile is much easier. At first, for each slice the median distance value is computed. The set of all these median values is then called the *median profile*. Note that this profile is only virtual! Due to the averaging process on the median profile some meaningful details such as corner points might be levelled out. Hence, we only regard the profile that minimizes the pointwise Euclidean distance towards the median profile as the representative one. This optimal profile can serve for example for drawing documentation but also for an easier extraction of the measures from section 2.2.

## 3 Similarity Estimation

After having extracted a set of features that gives a good abstract representation of the vessel's shape, some intuitive but also objective similarity measurement has to be found. This section deals

with metrics for different kinds of features and a reasonable way to weight their importance.

### 3.1 Similarity of Single Values

Yet the comparison of two values of a single feature is not easy. The metric to be chosen depends on the level of measurement (nominal, ordinal, interval, ratio or count), the range of values and the meaning that might be associated to certain intervals. Hence, for each feature a different metric might be applied. We make four proposals.

$$\text{sim}(a, b) = \begin{cases} \min \left\{ \frac{a}{b}, \frac{b}{a} \right\} & \text{sgn}(a) = \text{sgn}(b) \\ 0 & \text{else} \end{cases} \quad (2)$$

This relational approach is only suited for features that are at least ratio-scaled, i.e. that have a non-arbitrary zero value. This applies to all absolute measures but not necessarily for ratios. For them in case of values of different sign a negative similarity would be computed.

In contrast, the metric induced by

$$\text{sim}(a, b) = \max \left\{ 0, 1 - \frac{|a - b|}{\delta} \right\} \quad (3)$$

is much less restrictive. Here the sign is irrelevant and the range of tolerance can be controlled by the parameter  $\delta$ . It can be chosen from the total range of values down to zero where it converges towards the Boolean approach (eqn. 5).

In the special case that intervals represent a certain nominal value we can choose

$$\text{sim}(a, b) = \begin{cases} 1 & a \in I, b \in I \\ 0 & \text{else} \end{cases} \quad (4)$$

which however is the same as mapping all values onto a nominal scale beforehand and using the following equation instead.

$$\text{sim}(a, b) = \begin{cases} 1 & a = b \\ 0 & a \neq b \end{cases} \quad (5)$$

The Boolean similarity metric is the strictest one of all. It should only be used for nominal features whose extraction is very robust and whose interpretation is out of question.

### 3.2 Importance of Features

No matter what features and metrics are chosen, for the total similarity the single similarities should be summed up in a convex combination.

$$SIM(A, B) = \sum_i \lambda_i \cdot sim(a_i, b_i) \quad \left( \sum_i \lambda_i = 1, \lambda_i \geq 0 \right) \quad (6)$$

The weights  $\lambda_i$  are though far from being obvious. Some features may be more important than others. Normally, the archaeological expert has a rough conception of how to choose them but they also depend on the underlying material and the intended purpose. As it has been shown in decision tree algorithms like ID3 and C4.5, features can be ranked by importance with respect to a known set of classes. This technique adapted from information theory should be very briefly introduced here for nominal features. For numerical features and further details cf. e.g. [Quinlan 1993].

Let  $X$  be a set of classes and  $E$  a set of entities each assigned to either class  $x \in X$ , then  $p(x)$  denotes the probability that some  $e \in E$  belongs to the class  $x$  which is the same as  $x$ 's relative frequency. From that we can define

$$H(E) = - \sum_{x \in X} p(x) \cdot \log_2 p(x) \quad (7)$$

as the *entropy* or the *average self-information* of a set of entities. Assume now that we have a set of features  $F$  that describes each of the entities. As shown by Quinlan [1993] one can define a unique test on any feature  $f \in F$  so that  $E$  is split into  $n$  subsets  $E_i$  depending on the particular test. In case of nominal features this test is trivially reduced to equality whereas on numerical features a threshold is chosen and the outcome is twofold. In either case this yields the a posteriori entropy

$$H_f(E) = \sum_{i=1}^n \frac{|E_i|}{|E|} \cdot H(E_i). \quad (8)$$

The *information gain* of a test applied to  $f$ , i.e. the difference of entropies before and after that test can thus easily be written as

$$IG(f) = H(E) - H_f(E). \quad (9)$$

Simply, our most important feature is the one that maximizes that difference. Unfortunately, the gain criterion favours tests with many outcomes, for which a normalization has to be found. This can be done by the so-called *split information*

$$SI(f) = - \sum_{i=1}^n \frac{|E_i|}{|E|} \cdot \log_2 \frac{|E_i|}{|E|} \quad (10)$$

and finally we have a normalized *gain ratio* by

$$GR(f) = \frac{IG(f)}{SI(f)}. \quad (11)$$

As it can be seen from table 1, both information gain and gain ratio perform quite well, but the information gain underrates some of the important structural features. The gain ratio criterion generally favours abstract features over indices and indices over absolute measurements what corresponds even more to our expectations. It is also notable that the overall shape feature directly induces the primary type in more than 97% of all cases meaning that only very few types are allowed to have a considerable variance of shape. All absolute measures have a contribution being close to zero, what is remarkable as well. Ironically they are usually the only ones that are denoted in today's archaeological documentation.

Information Gain		Gain Ratio	
overall shape	1.796	overall shape	0.972
rim index	1.250	# hold handles	0.741
h(main diameter)	1.117	h(main diameter)	0.625
main index	1.054	base index	0.595
base index	0.861	rim index	0.584
# hold handles	0.697	main index	0.578
shoulder index	0.605	# eyelet handles	0.570
# eyelet handles	0.494	shoulder index	0.351
total height	0.474	total height	0.310
volume	0.326	rim diameter	0.288
main diameter	0.295	base bulge	0.260
neck index	0.245	h(neck diameter)	0.260
rim diameter	0.244	volume	0.244
h(neck diameter)	0.235	main diameter	0.214
neck diameter	0.215	base diameter	0.210
base diameter	0.193	neck index	0.173
base bulge	0.175	neck diameter	0.133
neck height	0.069	neck height	0.079
# lugs	0	# lugs	0
# tabs	0	# tabs	0

**Table 1:** Comparison of information gain and gain ratio values

Once having ranked the features their contribution to a user-defined query can easily be computed. Be  $F$  again the set of features to be considered, then the similarity between two vessels  $A$  and  $B$  is finally

$$SIM(A, B) = \frac{1}{\sum_{f \in F} GR(f)} \sum_{f \in F} GR(f) \cdot sim(f_a, f_b). \quad (12)$$

#### Missing Values

Not every feature can be extracted on every type of vessel. For example bowls don't have a neck and therefore neither a neck diameter, nor neck length, nor neck index. Furthermore, often some vessel parts are missing. It is up to the user whether missing values are ignored or if their contributonal similarity is set to zero. For the computation of the gain values missing values do not pose a problem.

## 4 Results

We verified our method on about 300 complete or at least completely reconstructed vessels from the Bronze Age cemetery of Kötitz (Eastern Saxony). Although this Lusatian culture material has been well studied before (e.g. [Ender 2000; Puttkammer 2008]), so far a consistent typology does not exist. In order to derive a set of classes that is almost free from individual interpretation, we employed decision tree learners and neural networks [Hörr et al. 2008b]. After several steps of iterative refinement we could differentiate 20 primary types, eight of them special forms with very few members and about 35 secondary types. 20 features have been taken of which six have been nominal, seven absolute measures and seven ratios (table 1).

Some results of queries to our database are shown in table 2. Although all vessels have been crafted without a potter's wheel the ranking is intuitive and comprehensible for the very most types. Furthermore, the fact that the vast majority of the most similar vessels belongs to the same class as the queried one indicates that the underlying typology is very sophisticated yet. We assume that the

results improve even further on industrially manufactured ceramics such as Greek and Roman ware.

Independently, for the daily archaeological work many benefits arise:

- Classification schemes can be refined by supervised machine learning techniques,
- classification can even be performed without the existence of a classifier but only by the similarity values and class labels of the most similar vessels,
- attempts for a chronological morphology of types (type genetics) can be made,
- material from different groups and cultures can be compared more objectively, leading to more precise definitions and maybe revealing new relations between them,
- and finally moving of peoples and trading of goods can be retraced and verified with current knowledge.

## 5 Conclusion and Outlook

From the presented work it turns out that it is possible to find similar vessels very precisely only by means of their shape features. This new tool for quantifying similarity objectively will enable archaeologists to come much faster to reliable scientific conclusions, to improve existing typologies, and also to discover supra-regional coherencies by overcoming international language barriers and missing standards. Instead of matching entities only on the basis of their overall geometry, they are described and compared in terms of their features. There is no evidence that this approach may not work in other domains too, e.g. weapons, tools or trinkets.

















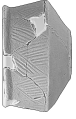











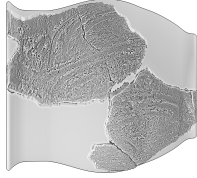

In the future we plan to set up a distributed retrieval system for pottery that also considers non-morphological features such as material, colour and burning [Wagner et al. 2008]. This system shall be based on specific ontologies and shall also allow tagging and textual description of objects. An interesting question to answer would be how accurate and reliable it is possible to date and classify an unknown vessel if the database contains material from many different eras.

## Acknowledgements

This work has been partially funded by the German Research Foundation (DFG) under item BR 1185/7-1. We like to thank the Archaeological Heritage Service of Saxony, in particular Elisabeth Lindinger for providing the data and giving us support on archaeological questions.

## References

- ADAMS, W. Y., AND ADAMS, E. W. 1991. *Archaeological typology and practical reality: a dialectical approach to artifact classification and sorting*. Cambridge University Press.
- ANKERST, M., KASTENMÜLLER, G., KRIEGEL, H.-P., AND SEIDL, T. 1999. 3D shape histograms for similarity search and classification in spatial databases. In *Proc. 6th International Symposium on Advances in Spatial Databases*, Springer, Hongkong, LNCS, 207–226.
- BIRKHOFF, G. D. 1933. *Aesthetic Measure*. Harvard University Press, Cambridge, Massachusetts, ch. IV, 67–86.
- BRENNECKE, A., AND ISENBERG, T. 2004. 3D shape matching using skeleton graphs. In *Simulation und Visualisierung*, SCS European Publishing House, Erlangen / San Diego, 299–310.
- BUSTOS, B., KEIM, D. A., SAUPE, D., SCHRECK, T., AND VRANIĆ, D. V. 2005. Feature-based similarity search in 3d object databases. *ACM Comput. Surv.* 37, 4, 345–387.
- CORNEA, N. D., DEMIRCI, M. F., SILVER, D., SHOKOUFANDEH, A., DICKINSON, S. J., AND KANTOR, P. B. 2005. 3D object retrieval using many-to-many matching of curve skeletons. In *Proc. Intl. Conference on Shape Modeling and Applications*, IEEE Computer Society, 368–373.
- ENDER, W. 2000. *Liebersee. Ein polykultureller Bestattungsplatz an der sächsischen Elbe*, vol. 2. Landesamt für Archäologie mit Landesmuseum für Vorgeschichte, Dresden.
- GILBOA, A., KARASIK, A., SHARON, I., AND SMILANSKY, U. 2004. Towards computerized typology and classification of ceramics. *Journal of Archaeological Science* 31, 681–694.
- HILAGA, M., SHINAGAWA, Y., KOMURA, T., AND KUNII, T. L. 2001. Topology matching for fully automatic similarity estimation of 3D shapes. In *Proc. SIGGRAPH*, 203–212.
- HÖRR, C., LINDINGER, E., AND BRUNETT, G. 2008. Considerations on technical sketch generation from 3D scanned cultural heritage. In *Proc. 36th Conference on Computer Applications and Quantitative Methods in Archaeology*, in press.
- HÖRR, C., LINDINGER, E., AND BRUNETT, G. 2008. New paradigms for automated classification of pottery. In *Proc. 36th Conference on Computer Applications and Quantitative Methods in Archaeology*, in press.
- KAMPEL, M., AND SABLATNIG, R. 2007. Rule based system for archaeological pottery classification. *Pattern Recognition Letters* 28, 740–747.
- MARA, H., SABLATNIG, R., KARASIK, A., AND SMILANSKY, U. 2004. The uniformity of wheel produced pottery deduced from 3d-image processing and scanning. In *Digital Imaging in Media and Education, Proc. 28th Workshop of the Austrian Association for Pattern Recognition (ÖAGM)*, 197–204.
- PUTTKAMMER, T. 2008. *Das prähistorische Gräberfeld von Niederkaina bei Bautzen*, vol. 10. Landesamt für Archäologie mit Landesmuseum für Vorgeschichte, Dresden.
- QUINLAN, J. R. 1993. *C4.5: Programs for Machine Learning*. Morgan Kaufmann.
- REUTER, M., NIETHAMMER, M., WOLTER, F.-E., BOUIX, S., AND SHENTON, M. 2007. Global medical shape analysis using the volumetric Laplace spectrum. In *Proc. Intl. Conference on Cyberworlds, NASA-GEM Workshop*, IEEE Computer Society, 417–426.
- RICE, P. M. 1987. *Pottery Analysis. A Sourcebook*. The University of Chicago Press, Chicago / London, ch. 7, 9.
- SARAGUSTI, I., KARASIK, A., SHARON, I., AND SMILANSKY, U. 2005. Quantitative analysis of shape attributes based on contours and section profiles in archaeological analysis. *Journal of Archaeological Science* 32, 841–853.
- WAGNER, S., HÖRR, C., BRUNNER, D., AND BRUNETT, G. 2008. What you give is what you get: Multitype querying for pottery. In *Proc. 36th Conference on Computer Applications and Quantitative Methods in Archaeology*, in press.
- WAGNER, S. 2007. *Ein Objekt-orientiertes Retrievalsystem für 3d-Modelle archäologischer Gefäße*. Diploma thesis (unpublished), Chemnitz University of Technology.
- WHALLON, R., AND BROWN, J. A., Eds. 1982. *Essays on Archaeological Typology*. Center for American Archeology, Evanston.

 Simple bowl	 0.981	 0.975	 0.967	 0.966	 0.966
 Profiled cup	 0.977	 0.976	 0.969	 0.967	 0.950
 Double-cone	 0.988	 0.971	 0.970	 0.967	 0.966
 Amphora	 0.970	 0.963	 0.957	 0.954	 0.950
 Storage vessel	 0.945	 0.938	 0.932	 0.931	 0.930

**Table 2:** Example queries and similarity values (all vessels scaled by 1:8)